Possibility of flux expulsion and flux trapping in thick mesoscopic cylinders

M. Czechowska,* M. Lisowski,† M. Szopa, and E. Zipper
University of Silesia, Institute of Physics, ul. Uniwersytecka 4, 40-007 Katowice, Poland
(Received 4 December 2002; revised manuscript received 2 May 2003; published 18 July 2003)

Persistent currents in mesoscopic nonsuperconducting rings and cylinders are a manifestation of quantum coherence. In this paper the possibility of self-sustaining persistent currents in thick mesoscopic cylinders is disscussed. The long-range magnetostatic (current-current) interactions are taken into account by the method of self-consistent field. Axially symmetric solutions of the differential equations for the self-consistent flux are found for geometry of a long hollow cylinder made of a set of a large number of cylindrical layers. The conditions under which the system exhibits flux expulsion and quantization of trapped flux are formulated.

DOI: 10.1103/PhysRevB.68.035320 PACS number(s): 73.23.−b, 73.63.−b

I. INTRODUCTION

It is well known that flux expulsion and flux trapping are one of the main features characterizing the superconducting state being a hallmark of a phase coherence.

In this paper we want to answer the question whether these phenomena can be obtained in nonsuperconducting structures such as metallic or semiconducting mesoscopic systems. We found that under very special conditions flux expulsion and flux quantization may exist in the normal state as well. Let us consider a mesoscopic cylinder of length L and wall thickness d,

$$d = R_2 - R_1, \tag{1}$$

(R_2 and R_1 are its outer and inner radii, respectively, $L \gg R_2$) in the presence of a magnetic field parallel to the cylinder axis. Because in the presented model considerations we do not invoke electron pairing to get a desired coherent behavior, one has to impose strong geometry and material requirements. The main difficulty with the normal multichannel structures is that, in general, different channels contribute with random sign to the response of the system. Thus, the main goal of this work was to find the realization in which all (or majority of) channels contribute with the same sign giving rise to the coherent behavior.

In this paper we perform some model calculations showing that flux expulsion and flux trapping can be obtained in mesoscopic cylinders of finite thickness with one-dimensional (1D) or two-dimensional (2D) conduction. Materials with layered structure where the conduction takes place in the layers or in the chains and also multiwall carbon nanotubes (MWNT) have the desired structure.

In mesoscopic systems the level quantization is mostly not due to the magnetic field (no Landau levels), but due to small sample dimensions. As a result, the wave function is rigid with respect to the magnetic field H and one can observe large orbital magnetism.[1] Cylindrical coordinates r, θ, and z shall be used, where r measures the distance from the cylindrical axis, θ is the angle around it, and z is the distance parallel to the axis.

Mesoscopic cylinders can exhibit diamagnetic or paramagnetic reaction to the small external magnetic field applied parallel to the cylinder axis. The induced currents are persistent at low T (Ref. 2) and, if their amplitude is high, there exists a possibility of creating self-sustaining currents that run even if we switch the external field off.[3,4] For simplicity we consider a system of spinless fermions. The generalization to the case with spin can be easily done. We also assume a relatively clean sample (ballistic regime) and we neglect the influence of disorder. The inclusion of weak disorder, which is known to decrease the amplitude of persistent currents, does not change the results qualitatively.

In our previous papers we discussed persistent self-sustaining currents[3,4] (fluxes) in mesoscopic hollow cylinders of radius R, length L, and a very small thickness d ($d \ll R$). The considerations were based on the assumption that the magnetic flux within the cylinder wall was practically constant and equal to $\phi = H\pi R^2$, where R was an external radius of a cylinder. In such thin samples we were not able to show the flux expulsion and the full flux quantization, but only some initial traces of it.

In this paper we remove the restriction of a very thin cylinder wall and consider cylinders with d smaller or of the order of R_1. The single quantity ϕ is then to be replaced by $\phi(r)$, measuring the flux contained within the radius r. Solving the differential equation for $\phi(r)$ one can formulate the conditions under which the mesoscopic system can exhibit full flux expulsion and trapping of the quantized flux. The results of our earlier papers were preliminary and only this paper gives the solution to the problem as the strong inhomogeneity of the flux is accurately accounted for. Below we discuss these phenomena in systems with quasi-1D and quasi-2D conduction. For simplicity we assume $T = 0$, the validity of the obtained results for finite T will be discussed in Sec. IV.

II. TOTAL ENERGY AND THE DIFFERENTIAL EQUATION FOR THE SELF-CONSISTENT FLUX

Let us consider a mesoscopic 3D cylinder made of a material with layered structure under the influence of a static magnetic field H. On the thickness d of the cylinder we have M_d coaxial closely packed layers ($d = M_d b$, b is the distance between layers) and the conduction takes place within the layers. Similar problem has been discussed in Ref. 5 for the mesoscopic system with $d \ll R_1$, where the difference in the radii of the layers has been neglected.

The field is partially of external origin and partially due to the currents in the system:

$$\mathbf{H}=\mathbf{H}_e+\mathbf{H}_i, \tag{2}$$

where $\mathbf{H}_e$ is the external magnetic field parallel to the cylinder axis and $\mathbf{H}_i$ is the magnetic field due to the currents in the system.

Because the conduction takes place only in the (z,θ) planes, internal field $\mathbf{H}_i$ produced by the electron motion and the total field $\mathbf{H}=\mathrm{curl}\,\mathbf{A}$ are parallel to the axis and depend only on r.

To study the coherent behavior of the system we use the method similar to that developed by Bloch and Rorschach[6] to study persistent currents in superconducting cylinders.

The energy of an electron system is given by

$$E_e=\sum_{j=1}^{M_d}\sum_{k_jl_j}N_{k_jl_j}\int_o^L dz\int_o^{2\pi}d\theta\Psi^*_{k_jl_j}\mathcal{H}_e\Psi_{k_jl_j}, \tag{3}$$

where $N_{k_jl_j}$ are the occupation numbers of electron states (kl) in a jth layer described by the normalized wave function $\Psi_{k_jl_j}$, $\mathcal{H}_e$ is the Hamiltonian operator for an individual particle

$$\mathcal{H}_e=\frac{1}{2m}\left(-i\hbar\boldsymbol{\nabla}-\frac{e}{c}\mathbf{A}\right)^2. \tag{4}$$

The state of an individual particle in a given layer can be characterized by the quantum numbers k and l, which, multiplied by $\hbar$, represent the components parallel to the z axis of linear and angular momentum, respectively. They are quantized due to the periodic boundary conditions applied in the θ and z directions.[6]

The corresponding wave function can be written in the form

$$\Psi_{kl}=\frac{1}{(2\pi L)^{1/2}}e^{i(kz+l\theta)}, \tag{5}$$

$$k=2\pi l/L,\quad l=0,\pm1,\pm2,\ldots.$$

Let ϕ_s be the flux inside the sth cylinder ($s=1,\ldots,M_d$), $s=1$ for the cylinder at $r=R_1$, $s=M_d$ at $r=R_2$. The flux[5] through the area between the $(s+1)$th and sth cylinders is created by $\mathbf{H}_e$ and $\mathbf{H}_i$, where $\mathbf{H}_i$ is the field created by the currents $I(\phi)$ in the outer cylinders. We get

$$\phi_{s+1}-\phi_s=2\pi r_s b\left[H_e+\frac{4\pi}{cL}\sum_{j=s+1}^{M_d}I(\phi_s)\right]\equiv 2\pi r_s b H_s. \tag{6}$$

Let us assume that ϕ_s is a smooth function of s. One can then transform Eq. (6) into a differential equation

$$H(r)=\frac{1}{2\pi r}\frac{d\phi(r)}{dr}, \tag{7}$$

where

$$\phi(r)=2\pi rA(r),$$

$$\phi=\phi_e+\phi_i, \tag{8}$$

ϕ_e and ϕ_i are the external and internal fluxes, respectively.

It has been shown[7] that the long-range magnetostatic (current-current) interactions when taken in the self-consistent mean-field approximation result in an internal magnetic flux ϕ_i.

Making use of Eq. (7) one can write down the formula for the energy stored in the magnetic field $H_i(r)$:

$$E_f=\frac{1}{8\pi}\int H_i^2(r)d^3r. \tag{9}$$

Replacing the sum over j in Eq. (3) by an integral, the expression for the total energy $E=E_e+E_f$ after some algebra takes the form

$$E=\frac{\pi L\hbar^2 n}{m}\int_{R_1}^{R_2}rdr\sum_{kl}\frac{N_{kl}}{N}\left[k^2+\frac{(l-\phi')^2}{r^2}\right]+\frac{L}{4}\left(\frac{\hbar c}{e}\right)^2\int_{R_1}^{R_2}\frac{1}{r}\left(\frac{d\phi_i'}{dr}\right)^2dr, \tag{10}$$

where N is the number of electrons in a single layer, $\phi'=\phi/\phi_0$, $\phi_0=hc/e$, ϕ_0 is the flux unit, $n=1/a^2b$ is the electron density, a is the lattice constant in the conducting planes. Notice that the flux ϕ' shifts the energy levels connected with the angular momentum leading to unequal (asymmetric) occupation of $\pm l$ states.

Equation (10) now be used to obtain the formula for the self-consistent flux. Demanding that the energy E has an extremum against variation of the function $\phi_i'(r)$ and using the standard Euler-Lagrange procedure we get the following equation for $\phi_i'(r)$:

$$r\frac{d}{dr}\left(\frac{1}{r}\frac{d\phi_i'}{dr}\right)=-\frac{4\pi e^2 n}{mc^2}\sum_{kl}\frac{N_{kl}}{N}(l-\phi'). \tag{11}$$

One can notice that ϕ_i' on the left side of Eq. (11) can be replaced by ϕ', because such a replacement merely adds a term corresponding to the derivatives of ϕ_e', which is 0 in the region of space considered here.

Now we want to determine the occupation numbers N_{kl} for the lowest-energy state. As our calculations are performed at $T=0$, we assume that electrons occupy the lowest quantized energy levels. Thus, the occupation numbers are chosen to be

$$N_{kl}=\begin{cases}1, & \text{for}(kl)\text{below the Fermi surface (FS)}\equiv(kl)_{occ}\\ 0, & \text{otherwise.}\end{cases} \tag{12}$$

The Euler-Lagrange equation (11) now takes the form

$$r\frac{d}{dr}\left[\frac{1}{r}\frac{d\phi'(r)}{dr}\right]=-\frac{1}{\lambda^2}[i_p(\phi')-\phi'(r)], \tag{13}$$

where

$$\frac{1}{\lambda^2}=\frac{4\pi e^2 n}{mc^2}, \tag{14}$$

λ is the parameter containing only the material constants, known as a penetration depth,

$$i_p(\phi')=\frac{\sum_{(kl)_{occ}} l}{N}. \tag{15}$$

It is easy to see that the right-hand side (rhs) of Eq. (13) is proportional to the current I in a single cylindrical layer, where

$$I=\frac{e\hbar N}{2\pi m r^2}[i_p(\phi')-\phi']. \tag{16}$$

This current screens the magnetic field and when it is strong it can lead to flux expulsion and trapping of the quantized flux. I is composed of the paramagnetic and diamagnetic parts. The diamagnetic reaction, described by the term linear in ϕ' exhibits a strong flux expulsion. However, the total reaction to ϕ' depends also on a paramagnetic term $i_p(\phi')$, which is a monotonic (nondecreasing) steplike function. When it is such that it cancels almost exactly the diamagnetic response (narrow and low steps) we end up with a very small net current. When, on the other hand, $i_p(\phi')$ has wide and high steps, then the net current becomes substantial and we get a strong reaction to ϕ'.

III. FLUX EXPULSION AND FLUX TRAPPING

It is well known[2,4b] that persistent currents in mesoscopic 2D cylinders depend strongly on the correlation of currents from different channels labeled by k i.e., on the shape of the FS. The most favorable situation is when the FS is flat, perpendicular to the angular momentum, the currents then add coherently and the resulting current is the strongest. With increasing curvature of the FS the current becomes smaller.

The following subsections deal with the solutions of Eq. (13) for several special cases.

A. Rectangular FS

We consider two different cases.

In the first case *the FS lies in the middle of the gap between the last occupied and the first unoccupied state* in the (lth) direction in the reciprocal (k,l) space. It is shown as a dashed line in Fig. 1 for $\phi'<1/2$. For a given ϕ' the following momentum states below the FS are occupied, $k=-k_F,-k_F+1,\ldots,k_F$, and $l=-l_F+l',-l_F+l'+1,\ldots,l_F+l'$, where l' is given by

$$l'=[\phi'+\tfrac{1}{2}], \tag{17}$$

$[x]$ is the integer part of x.

For a such Fermi surface the sums over k and l in Eq. (15) are independent and

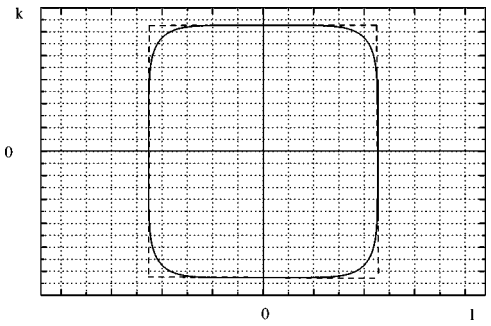

FIG. 1. Two shapes of the Fermi surface for which coherent behavior can be observed: rectangular and rectangular with rounded corners.

$$i_p(\phi')=\frac{1}{N}\sum_{k=-k_F}^{k_F}\sum_{l=-l_F+l'}^{l_F+l'} l=\frac{(2k_F+1)(2l_F+1)}{N}l'=l'. \tag{18}$$

Such cylinders exhibit a diamagnetic reaction to small ϕ. Current (16) is a sowtooth function with paramagnetic jumps at half integer ϕ' and diamagnetic in between. In fact, the number l' is the number of flux quanta (in units of ϕ_0) inside the cylindrical layer.

In the second case *the FS lies on the last occupied state* in the lth direction. In this case $-l_F+l'$ and l_F+l' states are only partially occupied and

$$l'=[\phi']+\tfrac{1}{2}, \tag{19}$$

i.e., the cylinders react with the paramagnetic jump at integer ϕ' being diamagnetic in between.

The Euler-Lagrange equation for the rectangular FS reads

$$r\frac{d}{dr}\left(\frac{1}{r}\frac{d\phi'}{dr}\right)=-\frac{1}{\lambda^2}(l'-\phi'). \tag{20}$$

Equation (20) is valid when all layers forming a thick cylinder exhibit the same (diamagnetic or paramagnetic) reaction to small ϕ'. The discussion of this condition is given in Sec. IV.

To solve Eq. (20) we denote

$$\beta(r)\equiv\phi'(r)-l', \tag{21}$$

$\beta(r)$ is proportional to the current I from Eq. (16).

Further we assume that in the considered range of r the value of l' is constant. This assumption is justified for the magnetic fields for which $|\beta(r)|\leqslant 1/2$.

Equation (20) takes now the form

$$r\frac{d}{dr}\left[\frac{1}{r}\frac{d\beta(r)}{dr}\right]=\frac{1}{\lambda^2}\beta(r). \tag{22}$$

By introducing a new variable x, $r=\lambda x$, and a function $y(x)$, where $\beta(r)=\lambda x y(x)$, Eq. (22) can be reduced to a form

$$x^2\frac{d^2y}{dx^2}+x\frac{dy}{dx}-(x^2+1)y=0. \tag{23}$$

It has well-known solutions $y(x)=c_1I_1(x)+c_2K_1(x)$ in terms of the modified Bessel functions of the first kind $I_1(x)$ and the second kind $K_1(x)$, c_1 and c_2 are constants. The general solution of Eq. (22) is thus of the form

$$\beta(r)=r\left[c_1I_1\left(\frac{r}{\lambda}\right)+c_2K_1\left(\frac{r}{\lambda}\right)\right]. \tag{24}$$

The constants c_1 and c_2 are to be found from the boundary conditions $\beta(R_i)=\phi'(R_i)-l'$, $(i=1,2)$, where $\phi(R_i)$ is the flux at the inner and outer wall of the cylinder, respectively.

In the limit $R_1,R_2\gg\lambda$, the Bessel functions can be well approximated by exponentials and solution (24) reduces to a simpler analytical form

$$\beta(r)=A_1\exp\left(-\frac{r-R_1}{\lambda}\right)+A_2\exp\left(\frac{r-R_2}{\lambda}\right). \tag{25}$$

We shall discuss now solution (25) in two limiting cases.[6]

1. Thin cylinder wall ($d\ll\lambda$)

We can expand $\beta(r)$ in powers of x/λ, where $x=r-R_1$. One obtains up to quadratic terms

$$\beta=A\left(1+\frac{x^2}{2\lambda^2}\right)+D\frac{x}{\lambda}, \tag{26}$$

where A and D are determined by the magnetic field $H(r=R_1)=H_1$ and $H(r=R_2)=H_2$.

From Eqs. (7) and (26) we obtain the relations for H_1 and H_2,

$$H_1=\frac{\hbar c}{eR_1}\frac{D}{\lambda}, \tag{27}$$

$$H_2=\frac{\hbar c}{eR_2\lambda}\left(\frac{Ad}{\lambda}+D\right). \tag{28}$$

We will consider now the case of trapped flux in the absence of an external magnetic field H_2. From $H_2=0$ one gets $A=-D\lambda/d$ and inserting it into Eq. (26) one finds

$$\beta(x=0)=-\frac{eR_1\lambda^2}{\hbar cd}H_1. \tag{29}$$

Making use of the relation $\Phi'(R_1)=\pi R_1^2H_1/\phi_0$, one obtains from Eq. (29) a self-consistent equation for $\phi'(R_1)$,

$$\phi'(R_1)=\frac{l'}{1+\frac{2\lambda^2}{R_1d}}, \tag{30}$$

where l' fulfills the condition $|l'|<(1+Rd/2\lambda^2)/2$.

In an analogous way we can calculate

$$\phi'(R_2)=\frac{l'\left(1+\frac{d}{R_1}\right)}{1+\frac{2\lambda^2}{R_1d}}\simeq\phi'(R_1)\quad(d\ll R_1). \tag{31}$$

Thus, the total flux contained in the cylinder is quantized, but the effective magnitude of the flux quantum (due to $d\ll\lambda$) is less than its full value ϕ_0.[8]

Equation (30) has a simple interpretation. Let us take, for example, the case with integer l' [Eq. (17)]. The inner layers carry current that creates a self-sustaining flux. However, for a very thin cylinder, if $Rd/2\lambda^2<1/2$, only $l'=0$ fulfills Eq. (30) and we cannot trap a flux, because the number of current carrying layers is too small. Formula (30) for the flux trapped in mesoscopic thin cylinders has been earlier obtained by us[4a] by a different method valid only for thin cylinders (we neglected the r dependence of the flux).

The investigations presented in this paper allow us to discuss the behavior of flux also in thick cylinders.

2. Thick cylinder wall ($d\gg2\lambda$, $R_1\gg\lambda$)

Inserting Eq. (25) into Eq. (7) one can express the constants A_1 and A_2 in terms of H_1 and H_2. After some algebra one obtains

$$\beta(r)\equiv\phi'-l'=\frac{2\pi\lambda}{\phi_0}(-R_1H_1e^{-(r-R_1)/\lambda}+R_2H_2e^{(r-R_2)/\lambda}). \tag{32}$$

One can see that this expression is appreciable only within distances of order λ from the boundaries of the cylinder and approaches 0 in its interior. As a result

$$\Phi'=l', \tag{33}$$

i.e., the quantized flux is trapped within the interior of the system.

Having solution for $\beta(r)$ one gets from Eq. (7) the formula for $H(r)$,

$$H(r)=\frac{\phi_0}{2\pi r}\frac{d\beta(r)}{dr}. \tag{34}$$

If we assume $H_1=H_2$ and $l'=0$ the exponential decay of $\beta(r)$ and $H(r)$ in the interior of the cylinder is equivalent to the flux expulsion, i.e., to the Meissner-like effect.

Figures 2–4 show $\beta(r)$ and $H(r)$ for different sets of parameters (λ,R_1,R_2).

In our model calculations we neglect tunneling between the sheets and, therefore, in metallic systems we assume $b\gg a$. In MWNT, although the distance between the walls is $b=3.4$ Å, tunneling is negligible because electrons are very strongly bound inside the walls.[9]

Assuming, e.g., $a=3$ Å, $b=19.1$ Å one finds from Eq. (14) $\lambda=694$ Å and by assuming the density n as for multiwall carbon nanotubes one gets $\lambda=160$ Å.

The solutions given by Eq. (24) are marked by the solid line and those given by Eq. (25) are marked by the dashed line. In Fig. 2 they almost coincide, whereas in Fig. 4 merely Eq. (24) is valid. We see that the magnetic field penetrates only to the depth of a few λ and is fully screened inside the cylinder wall if it is thick enough. This is the situation in Fig. 2 where $d\gg\lambda$ and we get full flux expulsion and flux quantization $\phi'=l'$.

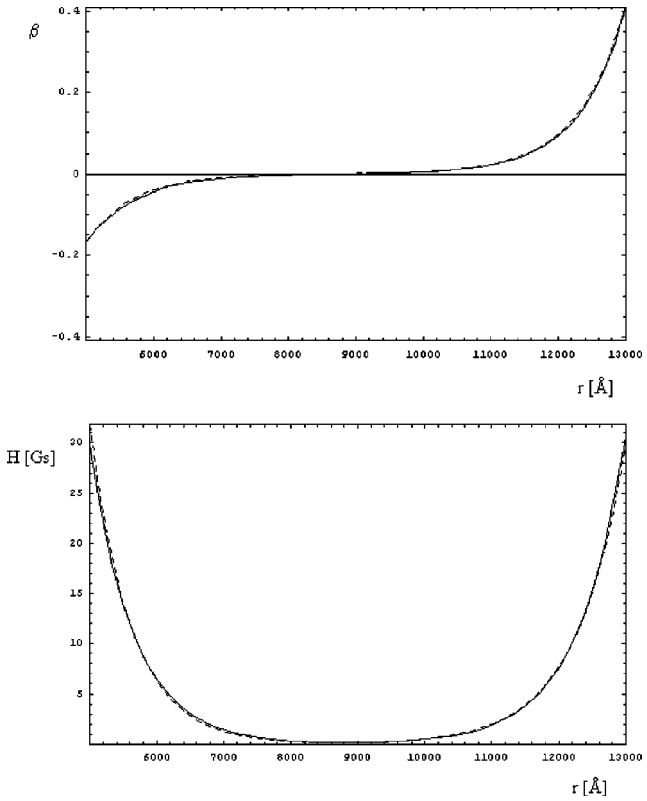

FIG. 2. Magnetic flux β and magnetic field H as a function of r for $R_1=5\times10^3$ Å, $R_2=13\times10^4$ Å, $\lambda=694$ Å.

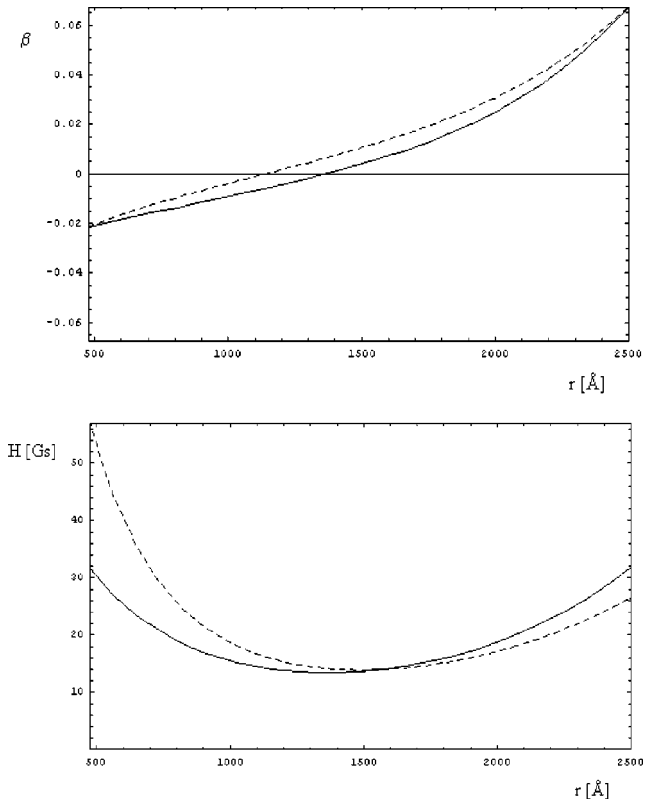

FIG. 3. Magnetic flux β and magnetic field H as a function of r for $R_1=478$ Å, $R_2=2500$ Å, $\lambda=694$ Å.

In Figs. 3 and 4 we observe only a partial flux expulsion due to the smaller width of the considered samples. The parameters in Fig. 4 are taken in the range typical for multiwall carbon nanotubes.

B. Circular Fermi surface

In the case of the circular FS, current (16) in each single sheet is very small (the paramagnetic and diamagnetic terms cancel almost exactly) and the rhs of Eq. (13) can be well approximated by 0,

$$r\frac{d}{dr}\left(\frac{1}{r}\frac{d\phi'(r)}{dr}\right)=0. \tag{35}$$

The solution of Eq. (35) is $\phi'(r)=H\pi r^2/\phi_0$, i.e., $H(r)=H$. In this case there is no flux expulsion, and the field penetrates into the mesoscopic cylinder.

C. Flat Fermi surface with rounded corners

The FS denoted by solid line in Fig. 1 contains two pairs of flat regions.

The sum over different k channels in Eq. (11) can be split into the part coming from the flat section and that of the rounded portion of the FS. In our considerations we neglect now the contribution to the current coming from the rounded part of the FS, as it is small (see above). We then calculate $i_p(\phi')$ coming from the channels in the flat section only. We obtain

$$i_p(\phi')\simeq fl', \tag{36}$$

where $f=M_{||}/M$, $f<1$, and $M_{||}$ is the number of channels in the flat section, $M=(2k_F+1)$.

Equation (20) is now replaced by

$$r\frac{d}{dr}\left(\frac{1}{r}\frac{d\phi'}{dr}\right)=-\frac{1}{\lambda_f^2}(l'-\phi'), \tag{37}$$

where $\lambda_f^2=\lambda^2/f>\lambda^2$. Equation (37) is of the same type as Eq. (20), but due to smaller number of coherent channels ($M_{||}<M$), the screening is weaker, which results in the larger penetration depth.

The discussion following Eq. (20) is also valid in this case with λ_f replacing λ.

For decreasing f the FS tends to the circular FS and the effect disappears for negligible f.

IV. DISCUSSION

We have considered a 3D mesoscopic cylinder made of a material with layered structure where the conduction takes place within the layers. If we apply the magnetic field H_e parallel to the cylinder axis, persistent currents are induced in the layers. The total magnetic field is then composed of H_e and the internal field H_i coming from the currents itself. The origin of H_i is the magnetostatic current-current interaction. As we consider the systems without electron pairing it was challenging to see what are the replacement conditions that have to be imposed to get the required coherent behavior.

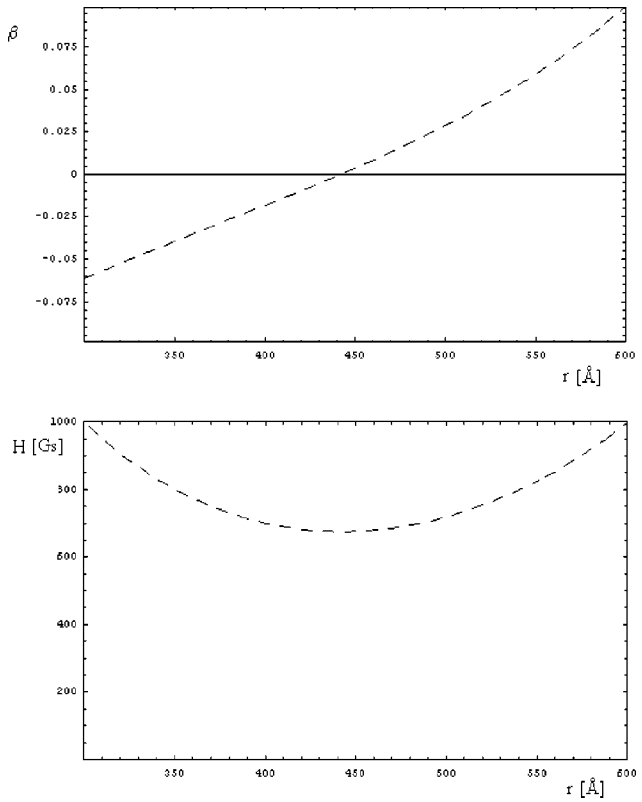

FIG. 4. Magnetic flux β and magnetic field H as a function of r for $R_1=300$ Å, $R_2=600$ Å, $\lambda=160$ Å.

It turned out that they are quite strong—the system has to exhibit quasi-1D or quasi-2D conduction and all (or majority of) the sheets have to react with the same (paramagnetic or diamagnetic) current to the small magnetic field.

We have estimated the geometric condition for which it happens. If $b=na/\pi$, n is an integer, then all sheets react with the same (e.g., diamagnetic) current to the small field. This is shown in Fig. 5 for the rectangular FS and for the FS with rounded corners. The inhomogeneity of the current (flux) inside the cylinder is also seen. Besides the geometric

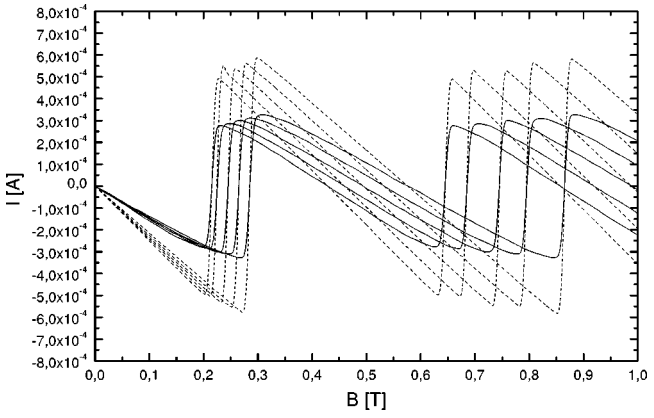

FIG. 5. The current I as a function of magnetic field B for the Fermi surfaces from Fig. 1 for five subsequent sheets with $r=R_1+sb$, $s=0,1,\ldots,4$, $R_1=478$ Å, $a=3$ Å, $b=19.1$ Å. Dashed line is for rectangular FS and solid line for FS with rounded corners.

condition we suppose that the interactions in the system can lead to such state if it minimizes the total energy. For example, the energy of the current-current interaction of the adjacent sheets is the smallest if the currents run in parallel. Such considerations would need to take into account many mechanisms together (including tunneling) and are outside our simple model calculations. This problem is interesting for further study.

For the circular FS the system exhibits a very weak reaction to ϕ followed by flux penetration and the absence of quantization.

We then considered the system whose FS has flat regions on its opposite sides. Such FS's are often met in low-dimensional systems,[10] e.g., in high-T_c superconductors, in organic materials, bcc and body-centered tetragonal crystals close to half filling, and in hole-doped carbon nanotubes.[11]

We have shown that systems with $d\gg 2\lambda$ and large f, i.e., with large number of channels in the flat section of the FS exhibit full flux expulsion and trapping of the quantized flux.

These coherent phenomena decrease with decreasing the thickness d of the cylinder, leading to partial flux expulsion and trapping of the quantized flux, but the effective magnitude of the flux quantum is then less than its full value [Eq. (30)].

The decrease in f leads to longer penetration depths.

The presented model calculations has been performed for simplicity at $T=0$. However, they are also valid for temperatures $T<T^*=\hbar v_F/2\pi^2 R_2$ for which persistent currents can be created in mesoscopic systems. The temperature dependence of persistent currents is given, e.g., in Refs. 2 and 4. Taking, e.g., $v_F=1.57\times 10^8$cm/s and $R_2=1\mu$m we get $T^*=0.6$K.

One can also estimate the upper magnetic field H^* for which the above considerations are valid. It can be calculated from the condition $\beta(R_2)=1/2$. By making use of Eq. (32) one gets

$$H^*=\frac{\phi_0}{4\pi R_2\lambda}. \tag{38}$$

The same formula for H^* can also be obtained if we equate the energy loss due to flux expulsion and the energy gain due to quantized flux (per single cylindrical sheet). Assuming, e.g., $R_2=1\mu$m, $\lambda=694$ Å, one finds from Eq. (38) $H^*=48$ Gs.

Notice that both T^* and H^* decrease with increasing R_2 and tend to 0 in the macroscopic samples. Thus, the presented phenomena can occur in samples of mesoscopic size.

In the presented model calculations we did not take explicitly into account the Coulomb interaction. It was recently shown that it does not influence persistent currents in clean systems,[12] whereas it enhances the currents in the diffusive regime.[13] In a work by Pascaud and Montambaux the experiments that permit to test the role of Coulomb interaction have been suggested.[14] One should also stress that although in the system considered by us the conduction is quasi-1D or -2D, the Coulomb interaction in such systems is 3D, which makes a nontrivial difference from the purely 1D case. The

Coulomb interaction hampers the fluctuations, which may destroy the ordering in a similar way as in bulk 3D systems.[15,16]

Mesoscopic cylinders with layered structure can also be obtained by, e.g., lithographic methods.[17]

MWNT consisting of a set of concentric sheets nested inside each other have also the desired cylindrical structure. However, in MWNT produced nowadays different sheets may have, in general, different chiralities, and thus different electric and magnetic behavior. Therefore, the assumption that the present paper is based on does not seem to be fulfilled. However, one can obtain such a sequence of sheets in MWNT that only some of them (e.g., every third sheet) exhibit strong persistent currents of the same type, whereas the others having different chiralities[18] give rise to the negligible current. Then the effective distance between the ''active'' sheets would be larger, but the idea remained the same.

The phenomena discussed in the presented paper are at the moment a theoretical prediction. However, with the rapid development of the nanotechnology used to fabricate low-dimentional structures, there is a hope that such materials will be fabricated in the future.

The Meissner-type effect and the orbital magnetism in clean cylindrical ring with $L,d<R$ have also been predicted in Ref. 19. Although the geometry of the system and the approximations used are different, in the presented paper the author also shows that at low T and at small magnetic field the nonsuperconducting system can show the quantized flux. Azbel considered a ring made of a bulk metal and to get coherent behavior he had to have very large cyclotron radius, and as a result his theory is valid at a magnetic field much smaller than in our case.

V. CONCLUSIONS

We have presented the model considerations that exhibit on a mesoscopic scale features similar to that of a superconducting state, such as the flux expulsion and trapping of the quantized flux although electron pairing was not invoked. The flux unit in the model is $\phi_0=ch/e$.

Quantum coherence is related here to both the small size of the sample (quantization due to the Quantum Size Effect) and to electron correlations coming from the magnetostatic interactions.

ACKNOWLEDGMENTS

This work was supported by Polish Committee for Scientific Research (KBN) Grant No. 5P03B0320. One of the authors (M.L.) thanks the Foundation for Polish Science (FNP) for financial support.

*Email address: cehovska@server.phys.us.edu.pl
†Email address: lisow@server.phys.us.edu.pl

[1] B. Shapiro, Physica A **200**, 498 (1993).
[2] H. Cheung, Y. Gefen, and E.K. Riedel, IBM J. Res. Dev. **32**, 359 (1988).
[3] D. Wohlleben, M. Esser, P. Freche, E. Zipper, and M. Szopa, Phys. Rev. Lett. **66**, 3191 (1991).
[4] (a) M. Szopa and E. Zipper, Int. J. Mod. Phys. B **10**, 161 (1995); (b) M. Stebelski, M. Szopa, and E. Zipper, Z. Phys. B: Condens. Matter **103**, 79 (1997).
[5] E.V. Tsiper and A.L. Efros, J. Phys. Condens. Matter **10**, 1053 (1998).
[6] F. Bloch and H.E. Rorschach, Phys. Rev. **128**, 1697 (1962).
[7] M. Lisowski, E. Zipper, and M. Stebelski, Phys. Rev. B **59**, 8305 (1999).
[8] J. Bardeen, Phys. Rev. Lett. **7**, 162 (1961).
[9] *Carbon Nanotubes: Synthesis, Structure, Properties and Applications*, edited by M.S. Dresselhaus, G. Dresselhaus, Ph. Avouris (Springer-Verlag, Berlin, 2001).
[10] D.S. Dessau *et al.*, Phys. Rev. Lett. **71**, 2781 (1993); Z.X. Shen *et al.*, Science **267**, 343 (1995); J. Ruvalds *et al.*, Phys. Rev. B **51**, 3797 (1995); D.M. King *et al.*, Phys. Rev. Lett. **70**, 3159 (1993).
[11] M. Marganska, M. Szopa, and E. Zipper, Phys. Lett. A **299**, 593 (2002).
[12] Y. Avishai and G. Braverman, Phys. Rev. B **52**, 12 135 (1995).
[13] R. Berkovits and Y. Avishai, Europhys. Lett. **29**, 475 (1995); V. Ambegaokar and U. Eckern, Phys. Rev. Lett. **65**, 381 (1990).
[14] M. Pascaud and G. Montambaux, Europhys. Lett. **37**, 347 (1997).
[15] A.T. Zheleznyak, V.M. Yakovenko, and I.E. Dzyaloshinskii, Phys. Rev. B **55**, 3200 (1997).
[16] I.E. Dzyaloshinski and E.I. Kats, Sov. Phys. JETP **28**, 178 (1969).
[17] See, e.g., O.G. Schmidt and K. Eberl, Nature (London) **410**, 168 (2001).
[18] M. Marganska, M. Szopa, and E. Zipper (unpublished).
[19] Mark Ya. Azbel, Phys. Rev. B **48**, 4592 (1993).